

Geochemical modelling, ionic ratio and GIS based mapping of groundwater salinity and assessment of governing processes in Northern Gujarat, India

Kumari Rina · Chander Kumar Singh ·
P. S. Datta · Neha Singh · S. Mukherjee

Received: 15 April 2012 / Accepted: 19 October 2012 / Published online: 10 November 2012
© Springer-Verlag Berlin Heidelberg 2012

Abstract In semi-arid/arid regions, groundwater is the major source of irrigation, drinking and industrial requirements, water salinity and shortage are major problems of concern. North Gujarat, India, is one such area where highly saline groundwater is generally ascribed to rapid increase of population, agriculture and industries induced decline in water table by unplanned abstraction of groundwater. However, no effort has been made to discriminate the natural and anthropogenic influences on groundwater salinity. In this brief background, the present study attempts to identify the factors and processes controlling the groundwater salinity in the area, based on ionic ratios in integration with various graphical methods, saturation indices and geographical information system. $\text{Na}^+/\text{Ca}^{2+} > 1$ indicates the deficiency of Ca^{2+} possibly due to CaCO_3 precipitation or ion exchange process. $\text{Na}^+/\text{Cl}^- > 1$ and $\text{SO}_4^{2-}/\text{Cl}^- \gg 0.05$ suggest salinization is mainly due to wastewater infiltration and/or due to irrigation water return flow. Sea water intrusion in coastal parts, vertical and lateral mixing of water and anthropogenic inputs are also responsible for salinization of groundwater. USSL diagram, Na%, sodium adsorption ratio, residual sodium carbonate and magnesium hazard

indicate unsuitability of groundwater for irrigation purposes. To prevent groundwater salinization, appropriate measures need to be taken to control further indiscriminate exploitation of groundwater for irrigation.

Keywords Groundwater · Salinity · Geochemical processes · Ionic ratio · Geochemical modelling · Saturation index · Gujarat

Introduction

In many semi-arid/arid regions, due to inadequate surface water supply groundwater serves as major source of requirements for irrigation, drinking water and industrial purposes. Therefore, availability of adequate quantity of good quality groundwater is a matter of concern. High evapotranspiration coupled with less rainfall leads to accumulation of excess salt in the soil root zone. In order to minimize soil salinization, when excess amount of water is added in excess of that required by crops it causes leaching of the salts with the infiltrating water down the soil profile, increasing the salt content in the groundwater (Rhoads and Loveday 1990). Hence, in these regions, salinity and sodicity of water are the major problems, which are directly or indirectly associated with the local or regional geological formations, climatic conditions, natural recharge mechanism and land use. In the areas adjacent to the coast, various other processes such as evaporite dissolution, downward seepage from surficial saline water, return flows of irrigation with sewage effluent, deep brines or upward flow of deep saline water and fossil seawater (Aunay et al. 2006; Pulido-Leboeuf et al. 2003; Vengosh et al. 1999; Yamanaka and Kumagai 2006) may also result in salinization of groundwater.

K. Rina · C. K. Singh · N. Singh · S. Mukherjee (✉)
School of Environmental Sciences, Jawaharlal Nehru University,
New Delhi 110067, India
e-mail: saumitramukherjee3@gmail.com

C. K. Singh
Department of Natural Resources, TERI University,
Vasant Kunj Institutional Area, New Delhi 110067, India

P. S. Datta
Indian Agriculture Research Institute, New Delhi 110012, India

The Gujarat State in western India is one such semi-arid area where groundwater in large part is affected by salinity/sodicity problems ($EC > 4,000 \mu\text{S}/\text{cm}$) (Misra and Mishra 2007). Over the years, the groundwater salinity problem in 12 coastal districts of Gujarat resulted due to salinity ingress from large-scale use of groundwater by farmers. A total of 2,542 villages are affected either by dynamic salinity or by inherent salinity. Besides the salinization of coastal aquifers, groundwater salinity has been also reported in other parts of Gujarat. In North Gujarat, rapid increase of industries, agriculture and population has induced unplanned abstraction of groundwater, causing decline of water table/piezometric surface at the rate of ~ 3 months/year. Water table has declined by 100–150 m in last few decades (Gupta and Deshpande 2004). An acute shortage of water is exacerbated by the inferior water quality in terms of salinity, ascribed to decline in water table. However, no effort has been made to understand the causes and discriminate the natural and anthropogenic influences on groundwater salinity. In this brief background, the present study attempts to identify the factors controlling the groundwater salinity using ionic ratio in integration with various graphical methods, saturation index and geographical information system (GIS).

Geohydrology and climate of the study area

The study area ($\sim 7,221 \text{ km}^2$; Fig. 1), covering northern Gujarat districts Ahmedabad, Mehsana, Gandhinagar, Kheda and Anand, is bounded in the north and northeast by the Aravalli hills; in the east, by a ridge separating it from the Mahi basin; in the south, by the Gulf of Cambay; and in the west, by a ridge separating it from the basins of minor streams draining into the Rann of Kutch. Sabarmati River and its tributaries is the main source of surface water in the area. Geologically the area comprises crystalline rocks of Archean age in the northern and northeastern parts while recent alluvial deposits cover the central and southern parts (Datta et al. 1980); and large part is occupied by thick quaternary continental deposits of fluvio-marine origin. Precambrian hard rocks, semi-unconsolidated mesozoic formations, tertiary formation and unconsolidated alluvial deposits form the aquifers in this area. In the north and northeast part of the area, the meta-sediments of Aravalli and Delhi super group, granites and basic intrusive of post-Delhi period, Himmatnagar sandstones and Deccan traps form hard rock aquifer with low yield. In the lithological formation quartzites, phyllites, slates and schists associated with Kumbhalgarh, Gogunda, Jharol and Lunawada group of rocks (Merh 1995) along with feldspar, quartz, granite, pegmatites, chalcedony, chrysolite, conglomerate cemented sandstone, basalt, laterite, calcrete nodules,

quartz, calc-silicate rocks (Srivastava et al. 2001; Tandon et al. 1997) are also present. The sandy layers forming aquifer horizons are seen to be laterally continuous and vertically interspersed with thin semi-permeable clay/silt layers that may not have lateral continuity over a large area. The recharge area is in the foothills of Aravalli Mountains and discharge area is in the Gulf of Cambay. Groundwater occur both in unconfined and confined conditions, and there is no hydraulic continuity of the phreatic aquifers. Due to high gradient and undulating topography, the run off is high, which limits the aquifer storage. The average annual rainfall in the area is about 600–800 mm. The southwest monsoon from mid-June to mid-September contributes nearly 91–94 % of annual rainfall.

Sampling and analytical procedures

Based on the topographic sheets and satellite image, the study area was divided into several grids ($5 \text{ km} \times 5 \text{ km}$). The locations of the sampling sites, recorded using global positioning system (GPS, Garmin), are shown in Fig. 1. Representative groundwater samples from 56 locations (equitably distributed geographically) from the aquifers adjacent to the Sabarmati River were collected at the end of September 2008, representing the post-monsoon period. Sixty-one samples from different locations were collected in May 2009, representing the pre-monsoon period. The land use/land cover (LULC) map of the area (Fig. 1) was prepared using LISS image of IRS P6, which shows that most of the area is crop land interspersed with fallow land.

Groundwater samples were collected from tube wells, bore wells and hand pumps. Initially water was discarded for 20–25 strokes from the hand pumps to minimize the impact of iron pipes. At each site, water samples were collected in two separate clean polypropylene bottles (Tarsons; 250 and 125 ml), rinsed two to three times with groundwater to be sampled. One of the bottles (125 ml) containing samples was acidified to stabilize trace metals and was used for determination of major cations and trace metals, and the other bottle (250 ml) containing un-acidified sample was used for anions' analysis. The physico-chemical parameters were determined by following the standard protocol as given in American Public Health Association (APHA 2005). pH, electrical conductivity (EC) and total dissolved solids (TDS) were measured onsite using respective electrodes (Hanna, model no. HI 99161). Subsequently, the samples were brought to laboratory in ice containing styrofoam boxes, vacuum filtered with 0.22μ Millipore filter paper, and stored at 4°C for further analysis. Carbonate and bicarbonate were determined using titration method. Anions (F^- , Cl^- , SO_4^{2-} , and NO_3^-) were analyzed using ion chromatography (ICS-90,

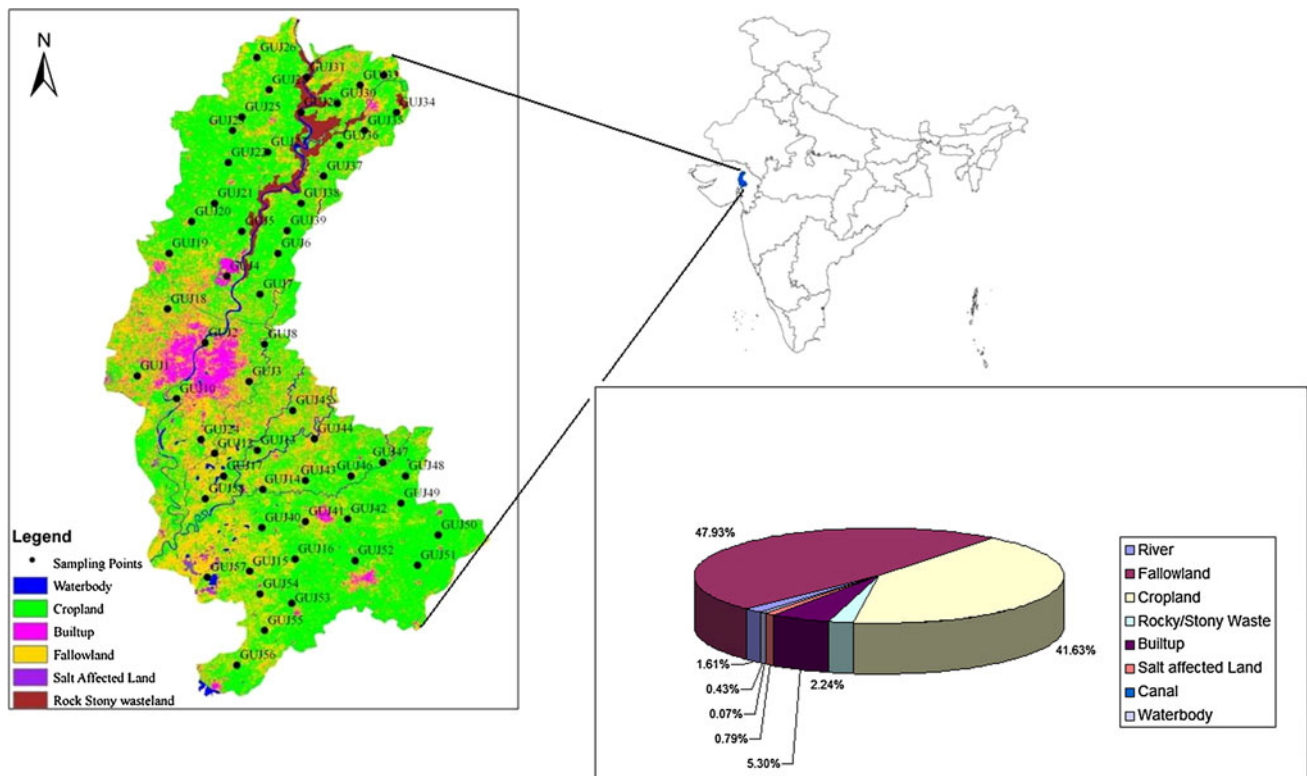


Fig. 1 Map showing sampling location with LULC of the study area

Dionex) and major cations (Ca^{2+} , Mg^{2+} , Na^+ , K^+) were analyzed using atomic absorption spectrophotometer (Thermo Fisher, M series). Dissolved silica was analyzed by molybdo-silicate method (APHA 2005). The analytical accuracy for measurement of ions was within $\pm 5\%$, as calculated by normalized charge balance index.

Durov’s diagram (1948) has been used to determine the hydrochemical facies of water, which are a function of lithology, solution kinetics and flow pattern of groundwater through the aquifer, and provide insight into the geochemical evolution of groundwater. The changes in saturation state has been used to distinguish different stages of hydrochemical evolution and to identify which geochemical reactions are important in controlling water chemistry (Koetsiers and Walraevens 2006). To evaluate the degree of equilibrium between water and the respective mineral, the saturation index (SI—ratio of apparent ionic product to apparent solubility product of the considered solid) of minerals was calculated by the USGS geochemical code PHREEQC 2.17 using the following equation (Garrels and Mackenzie 1967):

$$SI = \log\left(\frac{IAP}{K_t}\right) \tag{1}$$

where, SI is saturation index of a mineral, IAP = ion activity product of the dissociated mineral, K_t = equilibrium solubility at mineral temperature.

$SI < 0$ indicates that the groundwater is under-saturated with respect to a particular mineral. $SI > 0$ reflects whether the groundwater is oversaturated with respect to a particular mineral, i.e. incapable of dissolving more of the mineral.

Spatial analyst module of ArcGIS 9.1 was used to study spatiotemporal variation of the groundwater quality of the area. The inverse distance weighted (IDW) interpolation technique (Mueller et al. 2004; Tabios and Salas 1985; Tomczak 1998) has been used for estimating values between measurements. Weights have been computed by taking the inverse of the distance from an observation’s location to the location of the point being estimated (Burrough and McDonnell 1998). The inverse distance can be raised to a power (e.g. linear, squared and cubed) to model different geometries (e.g. line, area, volume) (Guan et al. 1999).

Results and discussion

The variation of anions and cations with their minimum, maximum and average concentration in pre- and post-monsoon is given in Table 1. The groundwater of the study area is alkaline in nature. The increase in groundwater pH from an average value of 7.49 in pre-monsoon to 8.43 in post-monsoon suggests enhanced dissolution of salt as a result of interaction between soil and rainwater (Subramanian and

Table 1 Statistical summary of different physico-chemical parameters analysed (concentration in mg/L except EC ($\mu\text{S/cm}$) and pH)

| Parameter | Pre-monsoon | | Post-monsoon | |
|------------------|----------------------|----------------|-----------------------|----------------|
| | Mean \pm SD | Range | Mean \pm SD | Range |
| pH | 7.49 \pm 0.39 | 7.1–9.1 | 8.43 \pm 0.40 | 7.1–9.3 |
| TDS | 884.75 \pm 458.19 | 160–1850 | 528.39 \pm 316.16 | 80–1,330 |
| EC | 1,258.2 \pm 725.31 | 210–2,890 | 1,307.68 \pm 607.81 | 240–2,350 |
| CO ₃ | 22.16 \pm 10.01 | 6.0–54.00 | 42.20 \pm 19.95 | 0–108.00 |
| HCO ₃ | 169.22 \pm 76.2 | 73.2–439.2 | 202.72 \pm 150.93 | 36.60–1,000.40 |
| SiO ₂ | 68.15 \pm 19.11 | 26.30–126.84 | 43.86 \pm 13.84 | 9.66–68.48 |
| F | 1.00 \pm 0.53 | 0.39–2.54 | 1.07 \pm 1.00 | 0.29–5.55 |
| Cl | 432.37 \pm 377.13 | 58.44–1,993.16 | 282.80 \pm 210.40 | 36.58–850.15 |
| NO ₃ | 50.09 \pm 87.49 | 1.59–630.73 | 33.28 \pm 29.12 | 2.71–131.67 |
| SO ₄ | 129.09 \pm 130.87 | 14.98–730.54 | 85.02 \pm 87.45 | 13.36–496.68 |
| Na | 374.76 \pm 199.05 | 90.01–1,050.34 | 321.07 \pm 187.75 | 63.89–808.36 |
| K | 3.38 \pm 2.59 | 0.54–12.41 | 2.69 \pm 1.91 | 0.46–10.21 |
| Ca | 20.56 \pm 12.23 | 1.87–58.86 | 27.32 \pm 14.66 | 10.19–80.17 |
| Mg | 13.49 \pm 18.54 | 0.87–128.67 | 22.66 \pm 12.75 | 2.42–62.41 |

Saxena 1983). High value of EC and TDS in pre-monsoon (warmer months) suggests enrichment of salt due to enhanced evaporation. Na⁺, Mg²⁺ and Ca²⁺ contributed 99.18 % of total cation whereas Cl⁻, HCO₃⁻ and SO₄²⁻ contributed 83.78 % of total anions in pre-monsoon. In post-monsoon Cl⁻, HCO₃⁻, and SO₄²⁻ contributed 83.15 % of total anions whereas Na⁺, Mg²⁺ and Ca²⁺ contributed 99.28 % of total cations. In both pre-monsoon and post-monsoon the abundance of major anions were in the order Cl⁻ > HCO₃⁻ > SO₄²⁻ > SiO₂⁻, whereas dominant cations followed the order: Na⁺ > Ca²⁺ > Mg²⁺ > K⁺.

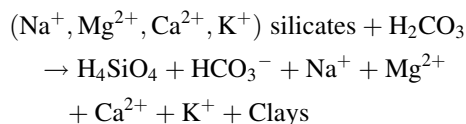
Hydrochemical facies

For identifying the processes such as mixing, cation exchange, and dissolution affecting groundwater composition, based on milliequivalent percentage of the total major cation and total major anions in the water samples, Durov's diagram (1948) for both pre- and post-monsoon is shown in Fig. 2a, b. The groundwater in the area is mostly of Na–Cl type, which is indicative of saline water. Very few places show Na–HCO₃ type facies, which confirms interaction of groundwater with schist quartzite and granitic rocks. In pre-monsoon only four samples are of Na–HCO₃ type and 58 are of Na–Cl type, whereas in post-monsoon 14 samples are of Na–HCO₃ type and 42 samples are of Na–Cl type.

Identification of geochemical process

Hydrochemical data was subjected to various graphical plots to identify hydro-geochemical processes responsible for enhancement of salinity in the region.

The scatter diagram of (Ca²⁺ + Mg²⁺) versus (HCO₃⁻ + SO₄²⁻) (Fig. 3a) shows that in pre-monsoon most of the samples fall below the equiline (1:1), which indicates that silicate weathering is the dominant process, whereas in post-monsoon more samples fall above the equiline due to excess of (Ca + Mg) over (SO₄ + HCO₃), which indicates that these ions have resulted from carbonate weathering, whereas some samples also fall below the equiline which indicates silicate weathering (Datta et al. 1996; Rajmohan and Elango 2004). It also indicates that in pre-monsoon ion exchange is the dominant process whereas in post-monsoon both ion exchanges as well as reverse ion exchange is taking place in the groundwater of the study area. Presence of granitic or gneissic environment causes dissolution of minerals yielding Ca²⁺, Mg²⁺, Na⁺ and K⁺ in groundwater as given in equation below.



In the scatter plot between (Na⁺ + K⁺) and Cl⁻ (Fig. 3b) in both pre- and post-monsoon almost all samples lie above the equiline suggesting the excess of cation is due to silicate weathering (Stallard and Edmond 1983). However, silicate weathering is not the only source of Na⁺ in groundwater, because, water that derives solutes primarily by silicate weathering would have HCO₃⁻ as the most abundant anion. Whereas, in the groundwater of the study area, HCO₃⁻ is the second most abundant anion after Cl⁻, hence, it shows the additional source of Na⁺ and Cl⁻. The additional sources of Na can be due to salt such Na₂SO₄ and K₂SO₄ present in the soil (Datta and Tyagi 1996). The observed excess of Na⁺ over K⁺ is because of the greater

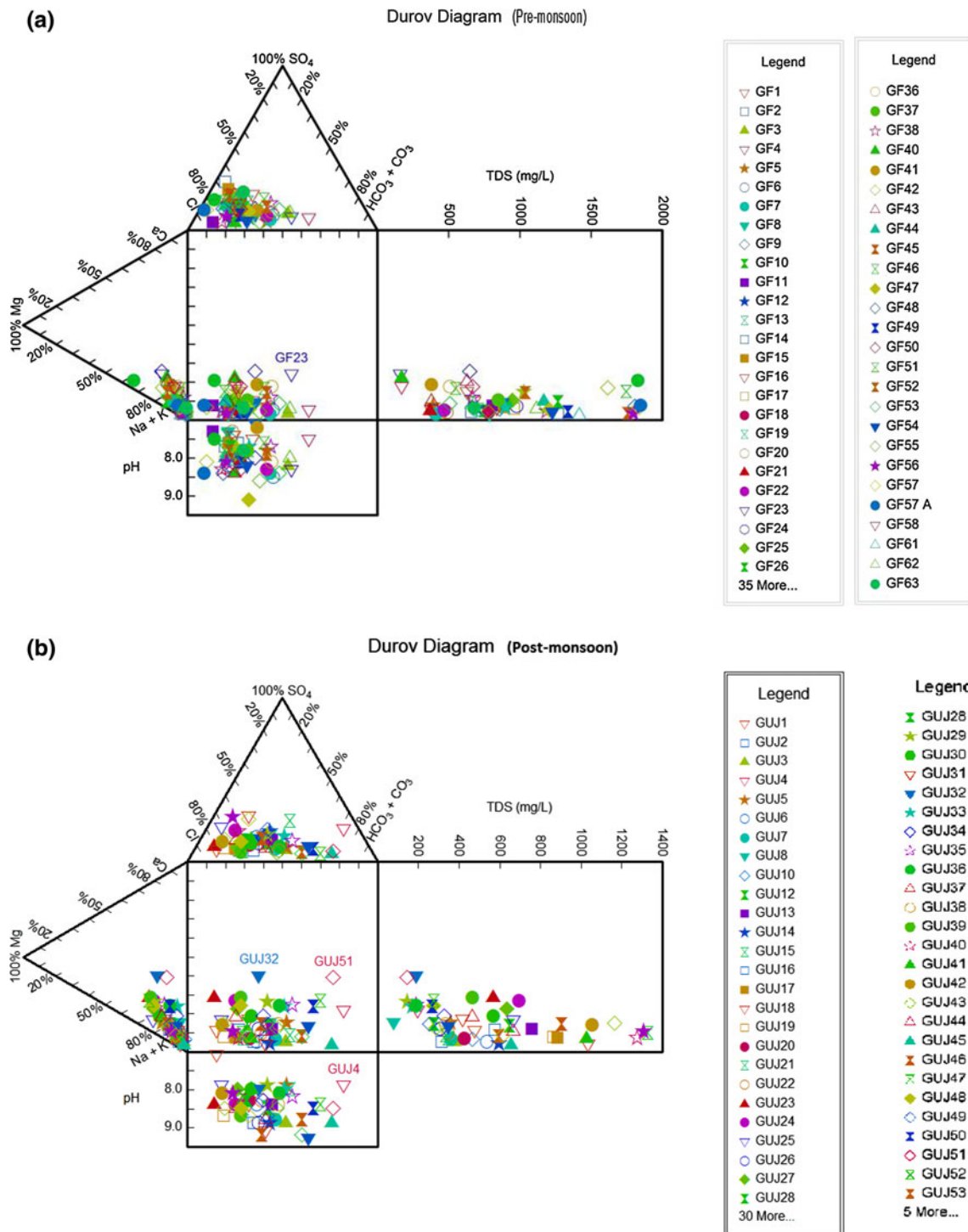


Fig. 2 Durov plot for **a** pre-monsoon, **b** post-monsoon

resistance of K^+ to chemical weathering and its adsorption on clay minerals. The scatter plot of $Na^+ + K^+$ versus Cl^- (Fig. 3b) shows that abundant alkalis are available to form alkali carbonates or alkali sulphate. Samples with high ($Na^+ + K^+$) concentration have high ($Cl^- + SO_4^{2-}$) concentration also, which suggests a common source of

these ions (Sarin et al. 1989, Datta et al. 1996). A good correlation of Cl^- and SO_4^{2-} ions in the scatter plot (Fig. 3c) suggests common source of these ions. The possible source of Cl^- and SO_4^{2-} could be relict sulphide and sulphate-rich marine clay and silt deposits, secondary evaporite minerals dissolution as well as anthropogenic

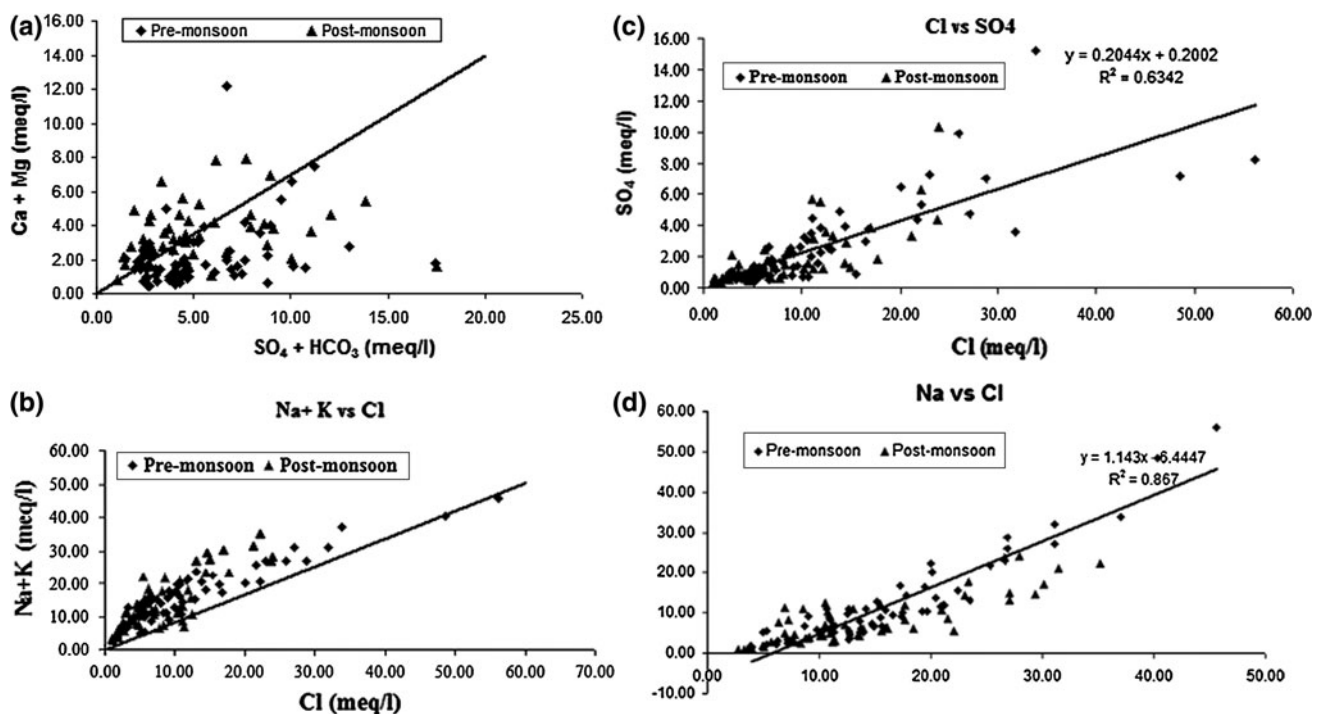


Fig. 3 a Scatter plot between $(\text{Ca}^{2+} + \text{Mg}^{2+})$ and $(\text{SO}_4^{2-} + \text{HCO}_3^-)$, b $(\text{Na}^+ + \text{K}^+)$ versus Cl^- , c Na^+ versus Cl^- , d Cl^- versus SO_4^{2-}

activities especially agricultural activities (Rajmohan and Elango 2006). Evaporation greatly increases the concentrations of ions formed by chemical weathering, leading to higher salinity (Subba Rao 2006). The Na^+ versus Cl^- scatter plot (Fig. 3d) suggests highly saline mixing of highly saline water with fresh water (Zaheeruddin and Khurshid 2004).

In the scatter plot of $(\text{Ca}^{2+} + \text{Mg}^{2+})$ versus $(\text{HCO}_3^- + \text{SO}_4^{2-})$, it is evident that in pre-monsoon the samples which fall below the equiline suggests that an excess of $(\text{HCO}_3^- + \text{SO}_4^{2-})$ in the water has been balanced by alkalis $(\text{Na}^+ + \text{K}^+)$. Whereas in post-monsoon even when SO_4^{2-} and HCO_3^- are at low concentration, Ca^{2+} and Mg^{2+} are present in relatively higher concentration which shows that the excess of Ca^{2+} and Mg^{2+} might be due to reverse ion exchange process which is taking place in the area in post-monsoon.

Ionic ratio and salinization

In general, freshwater is dominated by Ca^{2+} whereas seawater is dominated by Mg^{2+} ; along with sodium and chloride ions. However, seawater and seawater mixed with freshwater and freshwater polluted by various anthropogenic activities, urban wastewater or from agriculture return flow have distinguished chemical signatures (Ghabayen et al. 2006; Metcafe and Eddy 2000). Seawater has distinct ionic ratios also, such as, $\text{Na}^+/\text{Cl}^- = 0.86$, $\text{SO}_4^{2-}/\text{Cl}^- =$

0.05, $\text{Ca}^{2+}/(\text{HCO}_3^- + \text{SO}_4^{2-})$, $\text{Mg}^{2+}/\text{Ca}^{2+} = 5.2$ (Vengosh et al. 2002; Vengosh and Rosenthal 1994). Sewage effluent has a relatively high Na^+/Cl^- ratio (>1) and a high $\text{SO}_4^{2-}/\text{Cl}^-$ ratio (0.09) (Ghabayen et al. 2006; Vengosh et al. 1999). Improper treatment and disposal of domestic wastewater could be also one of the major sources of salinization in aquifer (Metcafe and Eddy 2000). Therefore, probable source of salinization can be also characterized by distinguishable ionic ratios in groundwater, controlled by processes such as preferential adsorption and ion exchange of cations on clay minerals, besides dissolution. Table 2 gives ionic ratios in groundwater of the study area for both pre- and post-monsoon periods.

At all the sampling locations, both in pre- and post-monsoon, $\text{Na}^+/\text{Ca}^{2+}$ molar ratios more than unity in groundwater indicates the deficiency of Ca^{2+} , possibly due to evaporation leading to formation of Kankar (CaCO_3) (Datta and Tyagi 1996; Subba Rao 2008; Singh et al. 2011a, b) or oversaturation of CaCO_3 or ion exchange process. In pre-monsoon, 52 samples had Na^+/Cl^- ionic ratio greater than 1. In post-monsoon, 51 out of 56 samples showed Na^+/Cl^- ratio more than 1 whereas 5 samples showed <0.8 . At most of the locations, $\text{Na}^+/\text{Cl}^- > 1$ indicates salinity of groundwater is mainly due to wastewater infiltration (Vengosh et al. 1999). In pre-monsoon, some of the samples in southernmost part of the area near Gulf of Cambay have a 0.8–1.0 Na^+/Cl^- ratio indicating possibilities of seawater intrusion due to overexploitation

Table 2 The comparative ionic ratio of potential salinization sources and study area groundwater

| Parameter | Seawater intrusion | Deep saline upconing | Agriculture return flow | Wastewater infiltration | Pre-monsoon | Post-monsoon |
|--|----------------------|-----------------------|-------------------------|-------------------------|-------------|--------------|
| Na ⁺ /Cl ⁻ | 0.86–1 ^a | <0.8 ^b | – | 1.1 ^c | 0.81–3.71 | 0.616–4.069 |
| SO ₄ ²⁻ /Cl ⁻ | 0.05 ^{a, c} | ~0.05 ^{b, c} | ≥0.05 ^d | 0.09 ^c | 0.057–0.450 | 0.082–0.734 |
| K ⁺ /Cl ⁻ | 0.019 | <0.019 ^c | – | ≥0.02 | 0.01–0.064 | 0.002–0.119 |
| Mg ²⁺ /Ca ²⁺ | >5 ^b | >1 ^a | – | – | 0.129–7.290 | 0.351–3.058 |

^a Vengosh and Rosenthal (1994)

^b Vengosh and Ben-Zvi (1994)

^c Vengosh et al. (1999)

^d Vengosh et al. (2002)

Table 3 Correlation matrix of various parameters analysed in pre-monsoon season

| | pH | TDS | EC | CO ₃ | HCO ₃ | SiO ₂ | F | Cl | NO ₃ | SO ₄ | Na | K | Ca | Mg |
|------------------|--------|--------------|--------------|-----------------|------------------|------------------|--------|--------------|-----------------|-----------------|-------|--------------|--------------|-------|
| pH | 1 | | | | | | | | | | | | | |
| TDS | 0.038 | 1.000 | | | | | | | | | | | | |
| EC | -0.050 | 0.929 | 1.000 | | | | | | | | | | | |
| CO ₃ | 0.319 | 0.207 | 0.200 | 1.000 | | | | | | | | | | |
| HCO ₃ | -0.028 | 0.119 | 0.198 | 0.433 | 1.000 | | | | | | | | | |
| SiO ₂ | 0.079 | 0.027 | -0.034 | 0.017 | 0.010 | 1.000 | | | | | | | | |
| F | 0.147 | -0.045 | -0.018 | 0.393 | 0.414 | -0.095 | 1.000 | | | | | | | |
| Cl | 0.004 | 0.743 | 0.805 | 0.209 | 0.083 | -0.067 | 0.034 | 1.000 | | | | | | |
| NO ₃ | -0.072 | 0.324 | 0.340 | -0.171 | -0.244 | -0.108 | -0.186 | 0.218 | 1.000 | | | | | |
| SO ₄ | -0.138 | 0.571 | 0.631 | 0.221 | 0.064 | -0.094 | 0.152 | 0.796 | 0.163 | 1.000 | | | | |
| Na | 0.003 | 0.738 | 0.814 | 0.320 | 0.239 | -0.060 | 0.202 | 0.931 | 0.131 | 0.762 | 1.000 | | | |
| K | -0.038 | 0.346 | 0.234 | -0.205 | -0.226 | 0.002 | -0.224 | 0.233 | 0.491 | 0.184 | 0.142 | 1.000 | | |
| Ca | -0.005 | 0.321 | 0.313 | 0.011 | -0.106 | 0.125 | 0.026 | 0.457 | 0.157 | 0.349 | 0.306 | 0.221 | 1.000 | |
| Mg | -0.098 | 0.536 | 0.546 | -0.050 | -0.082 | -0.170 | -0.071 | 0.433 | 0.745 | 0.400 | 0.316 | 0.490 | 0.543 | 1.000 |

Bold shows moderate to strong correlation

induced lowering of groundwater table and mixing of seawater and freshwater (Vengosh and Rosenthal 1994). The Mg²⁺/Ca²⁺ ionic ratio greater than 5 is a direct indicator of seawater intrusion (Metcafe and Eddy 2000; Vengosh and Ben-Zvi 1994). In the studied area, the groundwater in 45 locations show higher Mg²⁺/Ca²⁺ ratio (>1) in post-monsoon as compared to that in 22 locations during pre-monsoon, suggesting saline water upconing is responsible for high salinity in the groundwater. At most of the locations, SO₄²⁻/Cl⁻ ≥ 0.05 indicates possibility of contribution from the application of gypsum fertilizers also due to irrigation return flows towards the salinity (Vengosh et al. 2002), while at some of the locations SO₄²⁻/Cl⁻ ratio (0.09) suggests the effect of effluent disposal contributing to salinity. K⁺/Cl⁻ ratio of 0.019 indicates seawater intrusion. K⁺/Cl⁻ < 0.019 at most of the locations in the area depicts saline upconing. At few locations, quite high K⁺/Cl⁻ ≥ 0.02 ratio suggests waste water infiltration. As compared to pre-monsoon higher K⁺/Cl⁻ ratio in post-monsoon indicates the possibilities of salt patches leaching from rainfall causing more salinity.

It has been already observed that Cl⁻, Na⁺, Mg²⁺ and SO₄²⁻ contents exhibit mutual positive correlation and correlate strongly with EC and TDS in both pre- and post-monsoon (Rina et al. 2012). Compared to pre-monsoon, Cl⁻, Na⁺ and Mg²⁺ are strongly correlated with EC in post-monsoon, possibly due to high mineralization. Correlation of SO₄²⁻ – Cl⁻, Mg²⁺ – Cl⁻, Mg²⁺ – SO₄²⁻, K⁺ – NO₃⁻ and K⁺ – Mg²⁺ indicates the impact of excessive use of fertilizer for agricultural activity which might have contributed towards increased salinity of groundwater in the region. Strong correlation of NO₃⁻ with Mg²⁺ in pre-monsoon and moderate correlation Ca²⁺–Mg²⁺ in post-monsoon suggests a common source of these ions. The likely source of enrichment of these ions could be evaporite dissolution or seawater ingress. Correlation matrix of both pre- and post-monsoon is given in Tables 3, 4.

Geochemical modelling

The variation in chemical composition of groundwater in an area is controlled by the evaporation, precipitation,

Table 4 Correlation matrix of various parameters analysed in post-monsoon season

| | pH | TDS | EC | CO ₃ | HCO ₃ | SiO ₂ | F | Cl | NO ₃ | SO ₄ | Na | K | Ca | Mg |
|------------------|--------|--------------|--------------|-----------------|------------------|------------------|--------|--------------|-----------------|-----------------|-------|--------------|--------------|-------|
| pH | 1 | | | | | | | | | | | | | |
| TDS | 0.038 | 1.000 | | | | | | | | | | | | |
| EC | -0.050 | 0.929 | 1.000 | | | | | | | | | | | |
| CO ₃ | 0.319 | 0.207 | 0.200 | 1.000 | | | | | | | | | | |
| HCO ₃ | -0.028 | 0.119 | 0.198 | 0.433 | 1.000 | | | | | | | | | |
| SiO ₂ | 0.079 | 0.027 | -0.034 | 0.017 | 0.010 | 1.000 | | | | | | | | |
| F | 0.147 | -0.045 | -0.018 | 0.393 | 0.414 | -0.095 | 1.000 | | | | | | | |
| Cl | 0.004 | 0.743 | 0.805 | 0.209 | 0.083 | -0.067 | 0.034 | 1.000 | | | | | | |
| NO ₃ | -0.072 | 0.324 | 0.340 | -0.171 | -0.244 | -0.108 | -0.186 | 0.218 | 1.000 | | | | | |
| SO ₄ | -0.138 | 0.571 | 0.631 | 0.221 | 0.064 | -0.094 | 0.152 | 0.796 | 0.163 | 1.000 | | | | |
| Na | 0.003 | 0.738 | 0.814 | 0.320 | 0.239 | -0.060 | 0.202 | 0.931 | 0.131 | 0.762 | 1.000 | | | |
| K | -0.038 | 0.346 | 0.234 | -0.205 | -0.226 | 0.002 | -0.224 | 0.233 | 0.491 | 0.184 | 0.142 | 1.000 | | |
| Ca | -0.005 | 0.321 | 0.313 | 0.011 | -0.106 | 0.125 | 0.026 | 0.457 | 0.157 | 0.349 | 0.306 | 0.221 | 1.000 | |
| Mg | -0.098 | 0.536 | 0.546 | -0.050 | -0.082 | -0.170 | -0.071 | 0.433 | 0.745 | 0.400 | 0.316 | 0.490 | 0.543 | 1.000 |

Bold shows moderate to strong correlation

climate, minerals present in geological formations, soil characteristics, hydro-geochemical processes, including dissolution, precipitation, ion exchange, sorption and desorption, together with the groundwater residence time

along the flow path and anthropogenic activity (Apodaca et al. 2002). This can be modelled by inverse geochemical approaches (Parkhurst and Appelo 1999). Variation of saturation index for different minerals of both pre- and

Fig. 4 Saturation index (SI) plot for **a** post-monsoon, **b** pre-monsoon

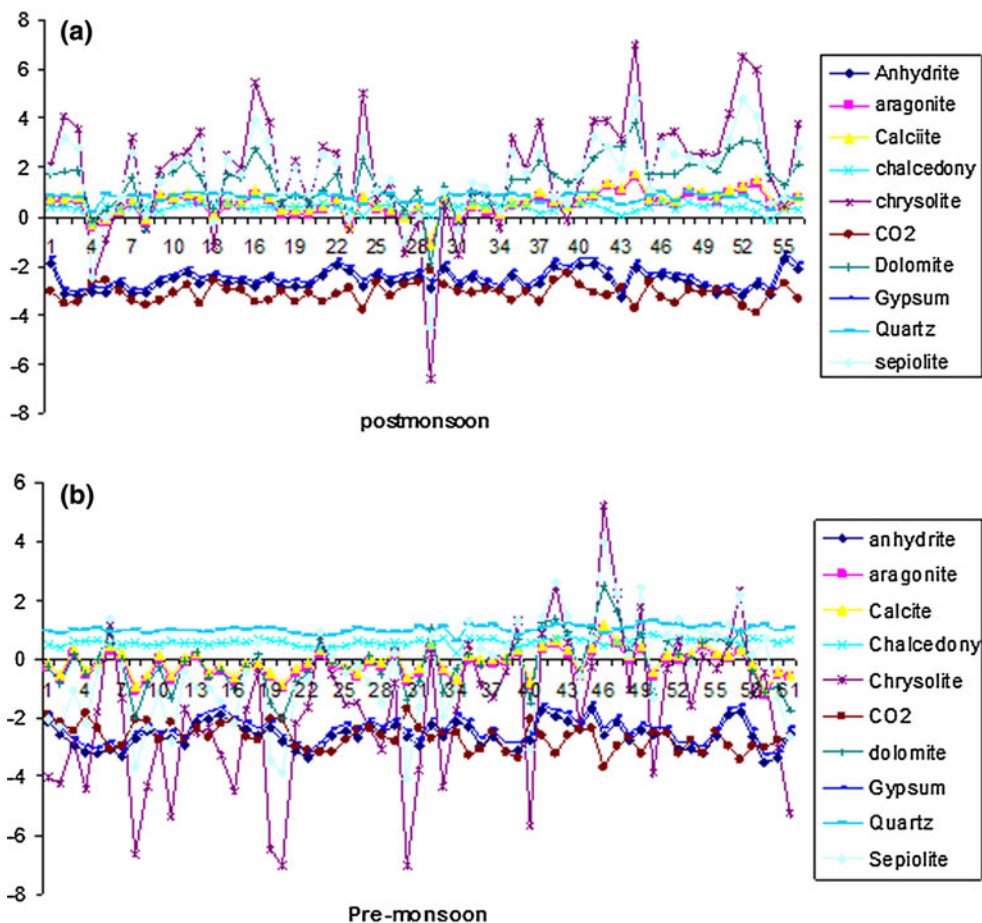


Table 5 Na% value of study area both in pre- and post-monsoon

| Na | Water class | Percentage of sample (pre-monsoon) | Percentage of sample (post-monsoon) |
|-------|-------------|------------------------------------|-------------------------------------|
| <20 | Excellent | 0 | 0 |
| 20–40 | Good | 0 | 0 |
| 40–60 | Permissible | 0 | 8.93 |
| 60–80 | Doubtful | 19.67 | 37.5 |
| >80 | Unsuitable | 80.33 | 53.57 |

post-monsoon is shown in Fig. 4a, b. Groundwater is under-saturated with respect to anhydrite, chrysolite, gypsum and CO₂ at most of the sampling sites both in pre- and post-monsoon; it suggests dissolution of these minerals have contributed Ca²⁺, Mg²⁺ and other ions in the groundwater. However, at most of the locations, groundwater is oversaturated in post-monsoon with respect to chrysolite. In post-monsoon most of the samples were found to be oversaturated with respect to calcite and dolomite. In pre-monsoon, 32 samples out of 61 samples were under-saturated with respect to calcite and 34 samples were under-saturated with respect to dolomite rest other

samples are oversaturated. Almost all the samples are oversaturated with respect to chalcedony in both pre- and post-monsoon. Oversaturation can be possibly produced by factors that include incongruent dissolution, common ion effect and evaporation (Appelo and Postma 1996; Langmuir 1997).

Oversaturation of groundwater with respect to calcite, dolomite and aragonite shows that these minerals have already precipitated in the past and are not contributing much of Ca²⁺ and Mg²⁺ in the groundwater. In scatter plot of Na⁺ versus Cl⁻, most of the samples lie above the equiline (1:1) for both pre-monsoon and post-monsoon (Fig. 3c), which suggests that besides halite dissolution and ion exchange, Na⁺ ion is contributed by anthropogenic sources also (Subba Rao 2008). Calcium has sources other than calcite, dolomite and aragonite; gypsum dissolution and anthropogenic input seems to be an important source of calcium enrichment in groundwater. Under-saturation of gypsum and anhydrite in pre- and post-monsoon suggests that the possible source of sulphate may be anthropogenic activity and relics of marine deposits as discussed above. The saturation indices for calcite, dolomite and gypsum and other minerals suggest that besides evaporites

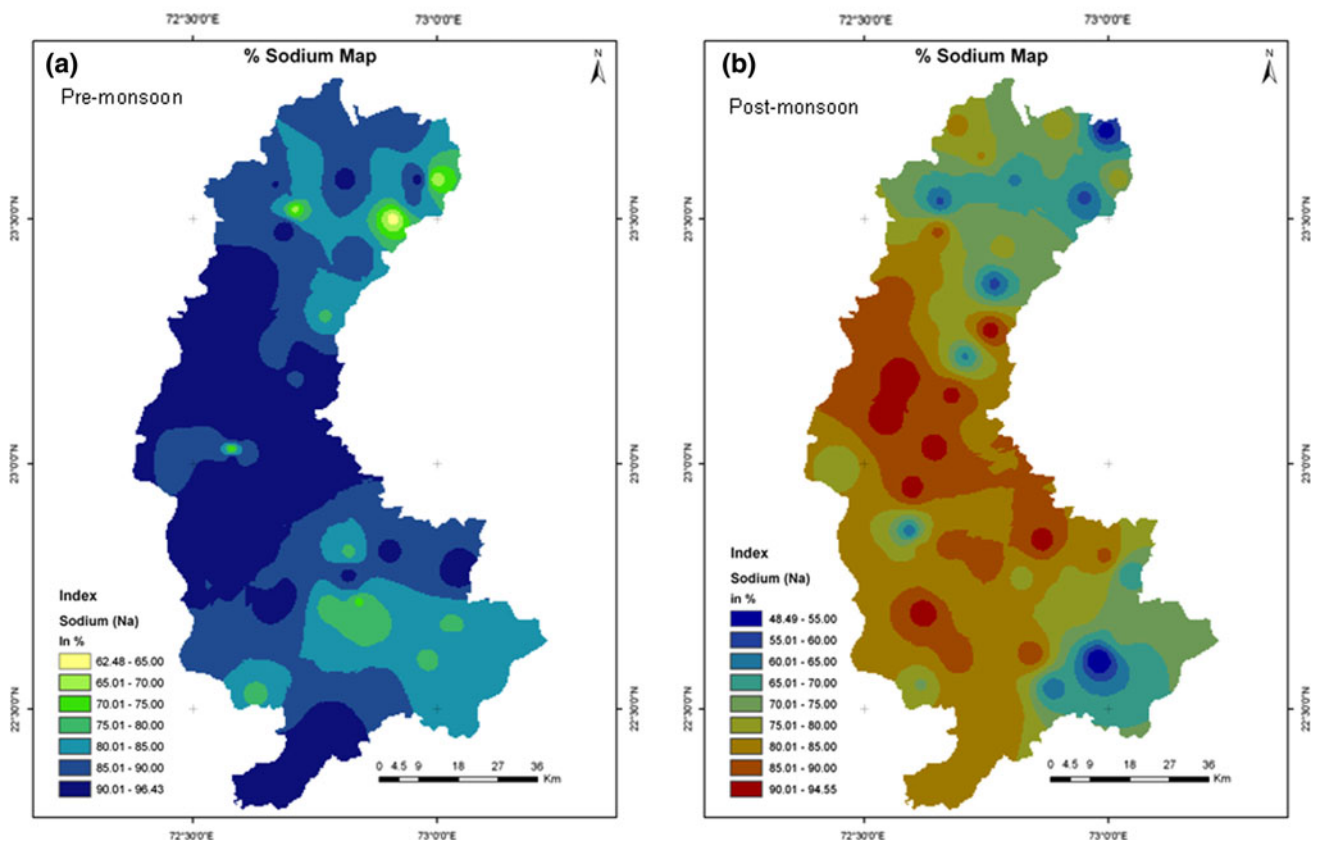


Fig. 5 Spatial distribution of Na% **a** pre-monsoon, **b** post-monsoon

Table 6 SAR value of study area both in pre- and post-monsoon

| SAR | Alkalinity hazard | Water class | Percentage of sample (pre-monsoon) | Percentage of sample (post-monsoon) |
|-------|-------------------|-------------|------------------------------------|-------------------------------------|
| <10 | S1 | Excellent | 21.31 | 48.21 |
| 10–18 | S2 | Good | 32.79 | 32.14 |
| 18–26 | S3 | Doubtful | 31.15 | 17.86 |
| >26 | S4 | Unsuitable | 14.75 | 1.79 |

dissolution and dedolomitization (calcite precipitation and dolomite dissolution driven by gypsum dissolution) and anthropogenic activities is controlling salinity of groundwater in this region.

In semi-arid/arid areas, use of such poor quality water again and again by farmers for irrigation causes adverse environmental impacts, such as, salinization of irrigated land, change in soil structure, permeability and aeration, increase in osmotic pressure of soil solution, decreasing water uptake of plant (Thorne and Peterson 1954; Singh et al. 2011a, b), indirectly affecting the plant growth (Todd 1980; Domenico and Schwartz 1990). Suitability of groundwater for irrigation depends on the constituents such as, EC and Na^+ , HCO_3^- and CO_3^{2-} . In this context, to determine the suitability of groundwater, indices such as

sodium percentage (Na%), sodium absorption ratio (SAR), residual sodium carbonate (RSC) and magnesium ratio have been also evaluated.

Sodicity and salinization of Groundwater

Sodium percentage (Na%)

The Na% has been calculated as:

$$\text{Na}\% = \frac{(\text{Na}^+ + \text{K}^+) \times 100}{(\text{Ca}^{2+} + \text{Mg}^{2+} + \text{Na}^+ + \text{K}^+)}$$

where, all the concentrations are expressed in meq/l.

In post-monsoon, Na% is less (48.45–94.55) compared to that in pre-monsoon (62.43–96.43), which may be due to increased vertical recharge from rainfall and lateral mixing with water containing less sodium concentration. Samples belonging to different class based on Na% in both pre- and post-monsoon are given in Table 5. Spatial variation of Na% in both the seasons is shown in Fig. 5a, b. Generally, Na% should not exceed 60 % in irrigation waters. All the samples are above the permissible limit in the pre-monsoon, which suggests unsuitability of water for irrigation. In post-monsoon, only some locations in the northern and southeastern parts are within permissible limit.

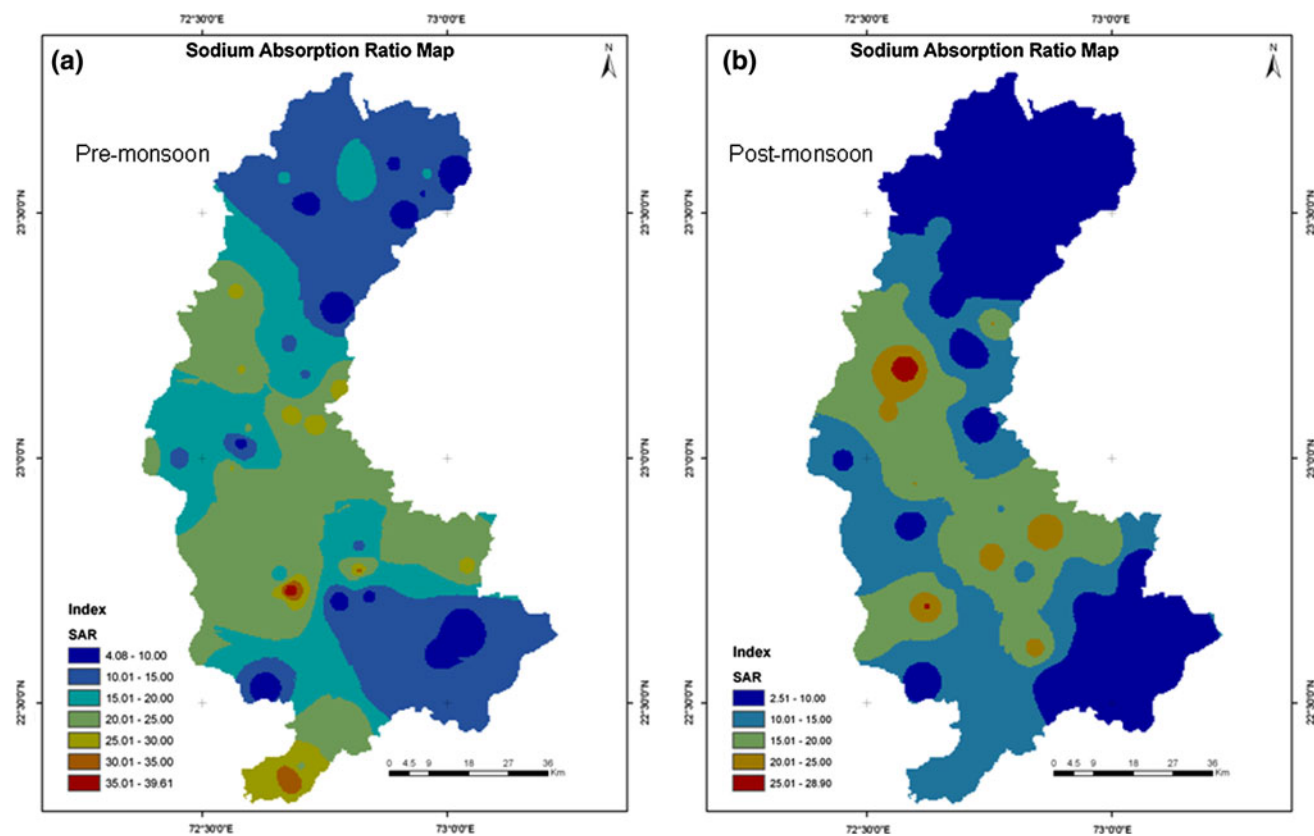


Fig. 6 Spatial distribution of SAR **a** pre-monsoon, **b** post-monsoon

Table 7 RSC value of the study area both in pre- and post-monsoon

| RSC | Water class | Percentage of sample (pre-monsoon) | Percentage of sample (post-monsoon) |
|----------|-------------|------------------------------------|-------------------------------------|
| <1.25 | Good | 44.64 | 50.00 |
| 1.25–2.5 | Doubtful | 34.43 | 19.64 |
| >2.5 | Unsuitable | 24.59 | 30.36 |

Sodium adsorption ratio

The extent to which sodium is adsorbed by the soils depends on SAR of irrigation water. SAR has been calculated as:

$$SAR = Na^+ / \sqrt{(Ca^{2+} + Mg^{2+})/2}$$

where, the concentrations are expressed in meq/l.

In pre-monsoon, SAR values varied from 4.04 to 39.72 (mean value 17.69) whereas in post-monsoon it varied from 2.50 to 28.92 (mean value 11.62). Samples belonging to different class based on SAR value in both pre- and post-monsoon are given Table 6.

As shown in Fig. 6a, b SAR is more pronounced in pre-monsoon than in post-monsoon. It is less in the northern

and southeastern parts and high in the central and southern parts of the study region.

Residual sodium carbonate

RSC has been calculated using the equation (Ragunath 1987):

$$RSC = (CO_3^{2-} + HCO_3^-) - (Ca^{2+} + Mg^{2+})$$

where, the concentrations are expressed in meq/l.

Water class of the study area based on RSC values for both pre- and post-monsoon is given in Table 7. In pre-monsoon the RSC value varied between -10.49 and 7.82 (mean 1.36) whereas in post-monsoon it varied between -3.47 and 16.82 (mean 1.48). A high value of RSC in water leads to increase in the adsorption of sodium in soil (Eaton 1950). Spatial variation of RSC in the region is shown in the Fig. 7a, b.

Compared to pre-monsoon, more area is affected by RSC in post-monsoon; especially in the region which is having relatively more urbanisation and industrial activities (Fig. 1), suggesting possible contribution by dissolution of higher amount of CO₂ released from industrial activity (Jeong 2001) during monsoon rainfall. From Fig. 7a we can clearly see that a very small area in the southernmost

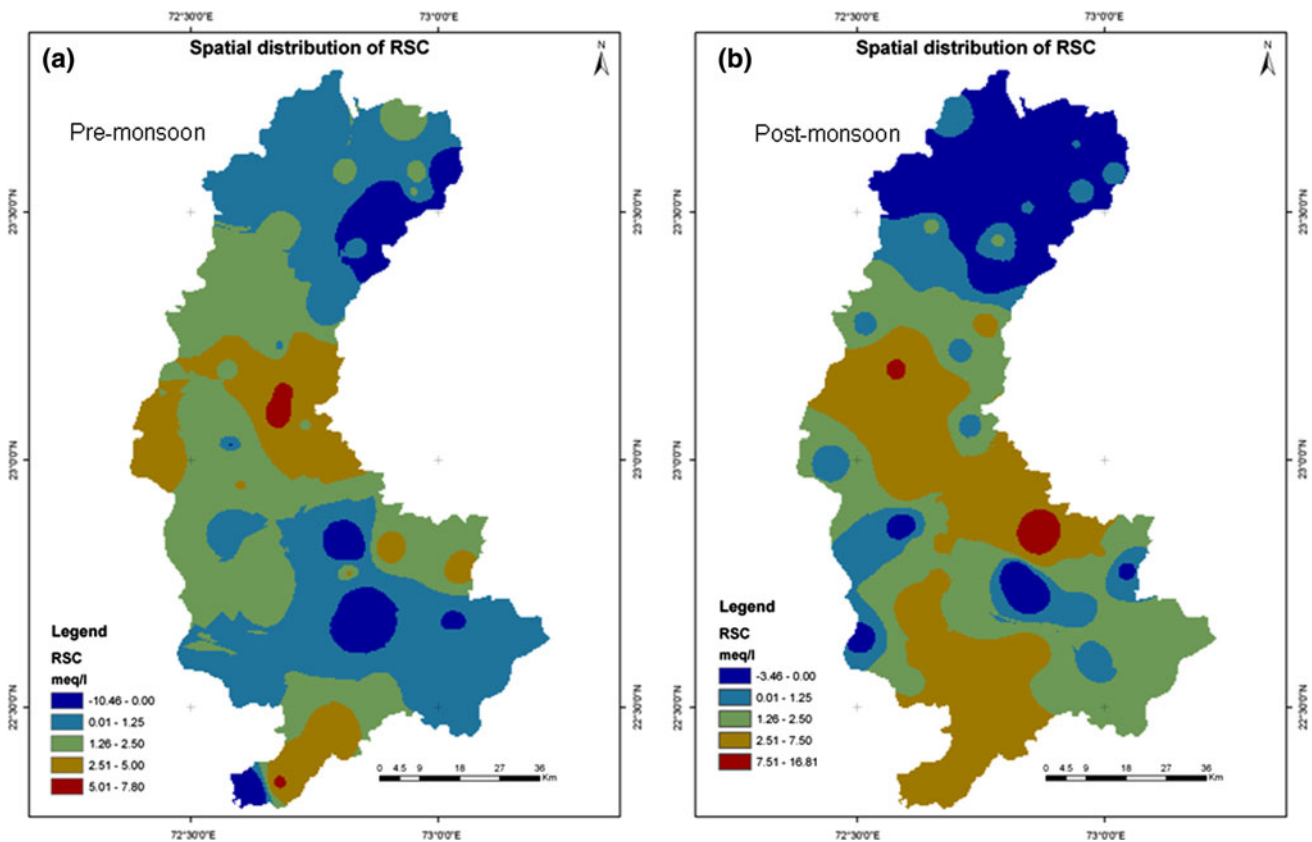


Fig. 7 Spatial variation of RSC a pre-monsoon, b post-monsoon

part, which is near the Gulf of Cambay and some parts of the central region were affected due to high RSC. In post-monsoon, two plumes of high RSC can be clearly identified in the southern and central part of the area moving towards the industrial hubs, which are Anand and Nadiad and its surrounding area. It suggests that because of overexploitation of groundwater in this region, saline water from the southernmost and central regions moves towards these regions and increases the salinity in this region.

Magnesium hazard (MH)

Generally, Ca^{2+} and Mg^{2+} maintain a state of equilibrium in water. If Mg^{2+} is more in water it adversely affects crop yield. Magnesium hazard for irrigation water has been calculated using the following equation (Szabolcs and Darab 1964):

$$\text{Magnesium ratio} = \frac{(\text{Mg}^{2+}) \times 100}{(\text{Ca}^{2+} + \text{Mg}^{2+})}$$

Spatial variation of magnesium hazard of study area is shown in Fig. 8a, b.

MH > 50 is considered harmful and unsuitable for irrigation purpose. In pre- and post-monsoon 23 and 45

samples were found to be unsuitable for irrigation respectively. In pre-monsoon, some parts in north, central and southeast of the study area show low magnesium ratio, whereas it is high in rest of the area. However, in post-monsoon almost all locations have high magnesium hazard except for some locations in northern and central parts. This is possibly due to increased leaching of salts by rain.

Wilcox (1955) and US salinity Laboratory Staff (1954) proposed a criterion for evaluating the suitability of water for irrigation. Both pre- and post-monsoon EC and SAR values of groundwater of the study area are plotted in the USSL salinity diagram in Fig. 9a, b, which indicate that in post-monsoon, 17 samples fall in low sodium hazard category. Most of the samples were in C3S2 (high salinity and medium sodium) category; however, it is considered tolerable for agricultural use. High salinity during post-monsoon might be due to increased leaching of surficial salt and untreated industrial waste with rainfall, along with salinity from remnant of the seawater (as discussed in the study area section above) (Merh and Chamyal 1993). The salinity diagram depicts different groundwater mixing flow pathways between highly saline and medium/low saline/fresh water.

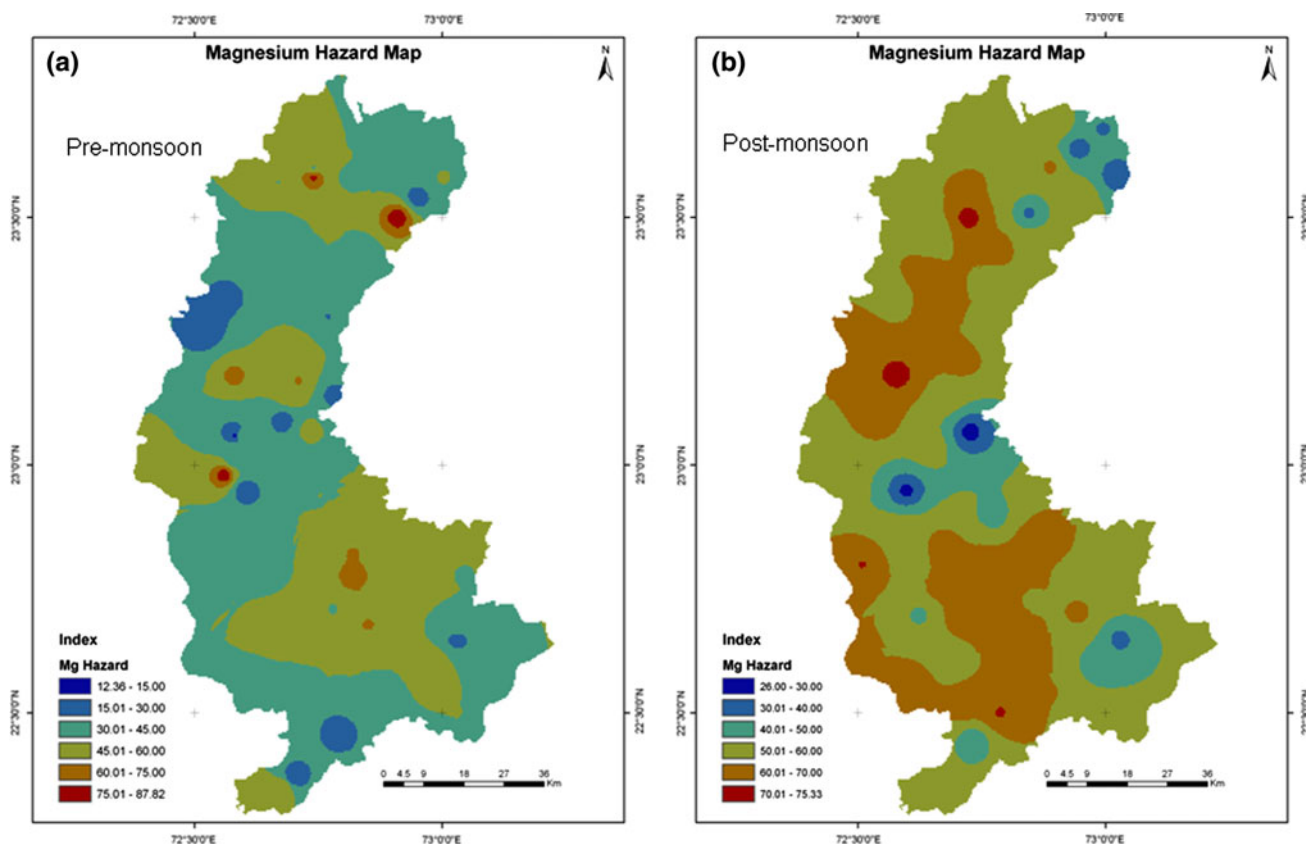
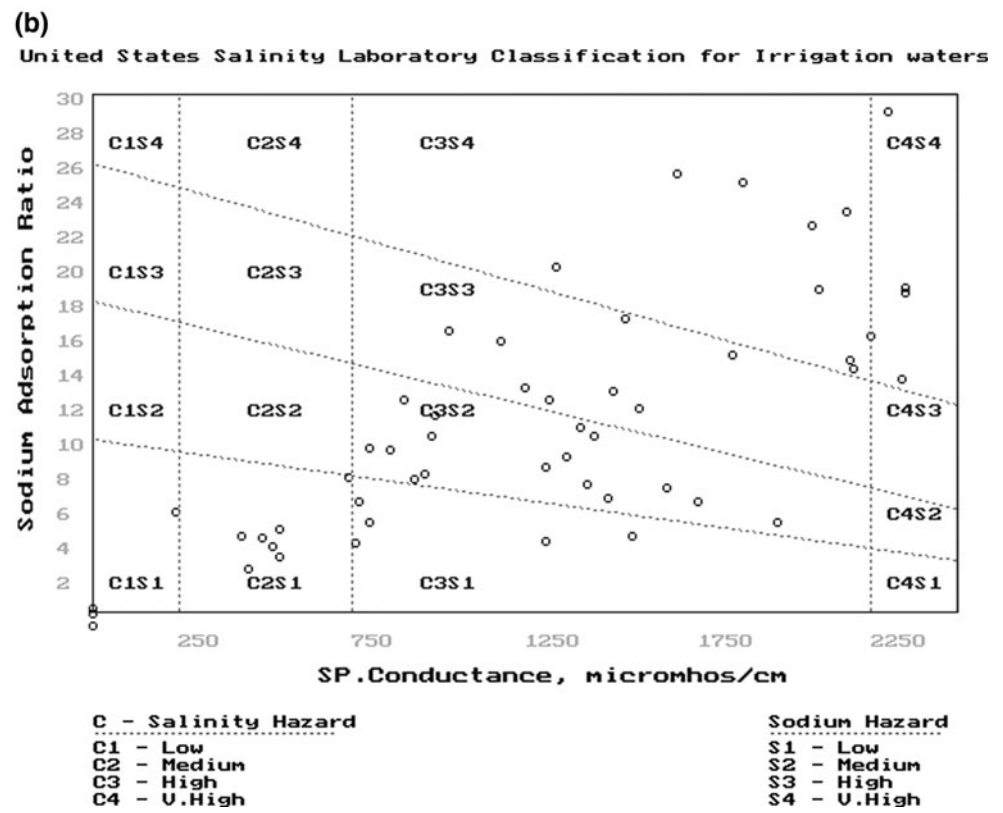
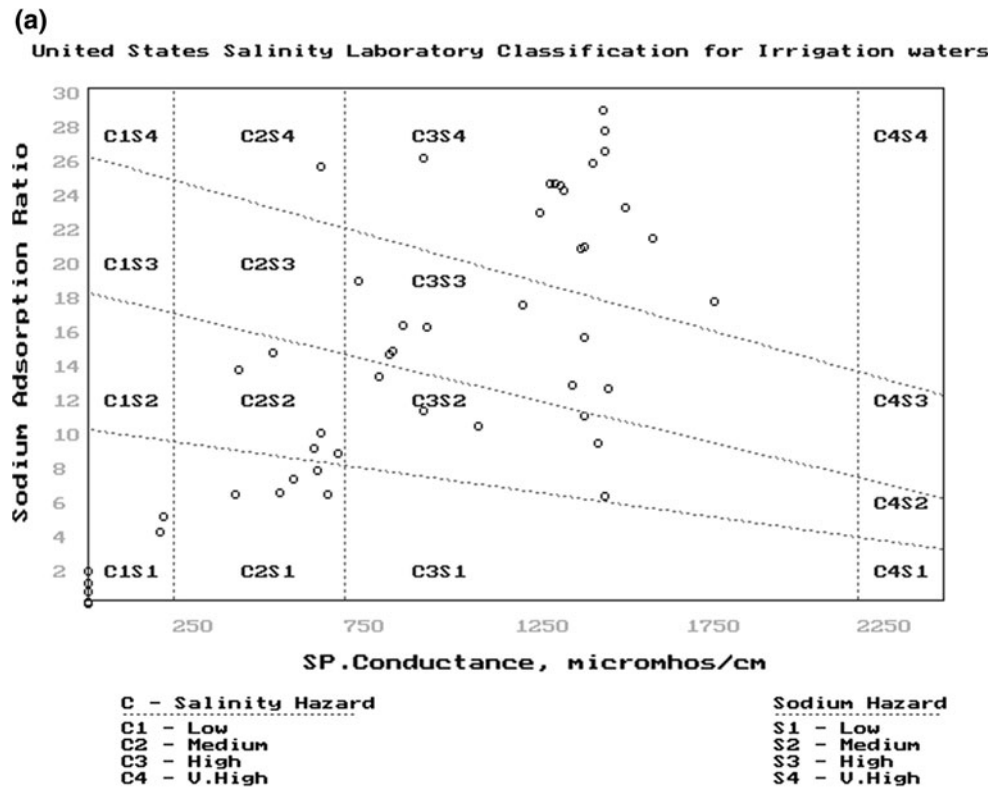


Fig. 8 Spatial variation of Mg Hazard **a** pre-monsoon, **b** post-monsoon

Fig. 9 US salinity diagram for **a** pre-monsoon, **b** post-monsoon



Conclusion

The integration of ionic ratio, hydrochemistry and various conventional graphs has helped to understand factors governing the groundwater salinity in the investigated area. Majority of the samples showed Na–Cl type hydrochemical facies, which indicates highly saline water. Various ionic ratios also confirm that along with natural processes, intensive agricultural and anthropogenic waste water infiltration from industrial activities are the major sources of salinization and the dominant processes which govern the groundwater salinity. However, ionic ratio confirms that in southernmost part near Gulf of Cambay, seawater intrusion is mainly responsible for salinity. Various indices such as Na%, SAR and RSC depict that water is unfit for agricultural purposes at most of the places. The salinity hazard is more pronounced in post-monsoon than pre-monsoon. It also depicts that due to overexploitation highly saline groundwater is getting mixed with fresh water and thereby depleting its availability. To prevent salinization of groundwater, appropriate measures need to be taken to control further indiscriminate and unplanned exploitation of groundwater and its application on agricultural land for irrigation.

Acknowledgments The author (Kumari Rina) acknowledges the anonymous reviewers for their comments, which have helped us to improve the manuscript. I also acknowledge the support from University Grants Commission for providing the fellowship to carry out this research. The author also thanks Jawaharlal Nehru University for providing various research facilities.

References

- American Public Health Association (APHA) (2005) Standard methods for the examination of water and waste water, 21st edn. American Public Health Association, Washington, DC
- Apodaca LE, Jeffrey BB, Michelle CS (2002) Water quality in shallow alluvial aquifers, Upper Colorado River Basin, Colorado. *J Am Water Resour Assoc* 38(1):133–143
- Appelo CAJ, Postma D (1996) *Geochemistry, ground-water and pollution*. Balkema, Rotterdam, p 536
- Aunay B, Dörfliger N, Duval C, Grelot F, Le Strat P, Montginoul M, Rinaudo JD (2006) Hydro-socio-economic implications for water management strategies: the case of Roussillon coastal aquifer. In: International Symposium—DARCYS, Aquifer Systems Management, Dijon
- Burrough PA, McDonnell RA (1998) *Principles of geographical information systems for land resources assessment*. Oxford University Press, New York
- Datta PS, Tyagi SK (1996) Major ion chemistry of groundwater Delhi area: chemical weathering processes and groundwater flow regime. *Geol Soc India* 47(2):179–188
- Datta PS, Desai DI, Gupta SK (1980) Hydrological investigations in Sabarmati basin. I. Groundwater recharge estimation using tritium tagging method. *Proc Indian Nat Sci Acad Part A* 46(1):84–98
- Datta PS, Bhattacharya SK, Tyagi SK (1996) ^{18}O studies on recharge of phreatic aquifers and groundwater flow-paths of mixing in the Delhi area. *J Hydrol* 176:25–36
- Domenico PA, Schwartz FW (1990) *Physical and chemical hydrology*. Wiley, New York 410
- Durov SA (1948) Natural waters and graphical representation of their composition. *Dokl Akad Nauk USSR* 59:87–90
- Eaton FM (1950) Significance of carbonates in irrigation waters. *Soil Sci* 39:123–133
- Garrels RM, Mackenzie FT (1967) Origin of the compositions of some springs and lakes. In: Stumm W (ed) *Equilibrium concepts in natural water systems*, vol 67. American Chemical Society, USA, pp 222–242
- Ghabayen SMS, McKee M, Kemblowski M (2006) Identification of salinity sources and missing data in the Gaza aquifer. *J Hydrol* 318:360–373
- Guan W, Chamberlain RH, Sabol BM, Doering PH (1999) Mapping submerged aquatic vegetation in the Caloosahatchee Estuary: evaluation of different interpolation methods. *Mar Geodesy* 22:69–91
- Gupta SK, Deshpande RD (2004) Water for India in 2050: first-order assessment of available options. *Curr Sci* 86:1216–1223
- Jeong CH (2001) Effect of land use and urbanization on hydrochemistry and contamination of groundwater from Taejon area, Korea. *J Hydrol* 253:194–210
- Koetsiers M, Walraevens K (2006) Chemical characterization of the Neogen aquifer, Belgium. *J Hydrogeol* 14:1556–1568
- Langmuir D (1997) *Aqueous environmental geochemistry*. Prentice Hall, Inc., New Jersey, p 601
- Merh SS (1995) *Geology of Gujarat*. Geol Soc India, Bangalore, p 220
- Merh SS, Chamyal LS (1993) The quaternary sediments in Gujarat. *Curr Sci Special Issue* 64:11–25
- Metcafe and Eddy (2000) Inc. Integrated Aquifer Management Plan: Final Report. Gaza Coastal Aquifer Management Program, USAID Contract No. 294-C-00-99-00038-00
- Misra AK, Mishra A (2007) Study of quaternary aquifers in Ganga Plain, India: focus on groundwater salinity, fluoride and fluorosis. *J Hazard Mater* 144:438–448
- Mueller TG, Pusuluri NB, Mathias KK, Cornelius PL, Barnhisel RI, Shearer SA (2004) Map quality for ordinary kriging and inverse distance weighted interpolation. *J Soil Sci Soc Am* 68:2042–2047
- Parkhurst DL, Appelo CAJ (1999) User's guide to PHREEQC (Version 2)—a computer program for speciation, reaction path, 1D-transport, and inverse geochemical calculations. USGS Water Resour Invest Rep 99-4259
- Pulido-Leboeuf P, Pulido-Bosch A, Calvache ML, Vallejos A, Andreu JM (2003) Strontium, $\text{SO}_4^{2-}/\text{Cl}^-$ and $\text{Mg}^{2+}/\text{Ca}^{2+}$ ratios as tracers for the evolution of seawater into coastal aquifers: the example of Castell de Ferro aquifer (SE Spain). *Comptes Rendus Geosci* 335:1039–1048
- Raghunath HM (1987) *Groundwater*. Wiley Eastern Ltd, Delhi, p 563
- Rajmohan N, Elango L (2004) Identification and evolution of hydrogeochemical processes in the groundwater environment in an area of the Palar and Cheyyar River Basins, Southern India. *Environ Geol* 46:47–61
- Rajmohan N, Elango L (2006) Hydrogeochemistry and its relation to groundwater level fluctuation in the Palar and Cheyyar River basins, southern India. *Hydrol Process* 20:2415–2427
- Rhoads JD, Loveday J (1990) Salinity in irrigated agriculture. In: Stewart BA, Nielsen DR (eds) *Irrigation of agricultural lands*, ASA Monograph No. 30. Am Soc Agro, Madison, pp 1089–1142
- Rina K, Datta PS, Singh CK, Mukherjee S (2012) Characterization and evaluation of processes governing the groundwater quality in

- parts of the Sabarmati basin, Gujarat using hydrochemistry integrated with GIS. *Hydrol Process* 26(10):1538–1551
- Sarin MM, Krishnaswami S, Dill K, Somayajulu BLK, Moore WS (1989) Major ion chemistry of the Ganga-Brahmaputra river system: weathering processes and fluxes to the Bay of Bengal. *Geochim Cosmochim Acta* 53:997–1009
- Singh CK, Shashtri S, Mukherjee S (2011a) Integrating multivariate statistical analysis with remote sensing and GIS for geochemical assessment of groundwater quality: a case study of Rupnagar District in Siwaliks of Punjab, India. *Earth Environ Sci* 62(7):1387–1405
- Singh CK, Kumari R, Singh RP, Shashtri S, Kamal V, Mukherjee S (2011b) Geochemical evidences of high fluoride concentration in groundwater of Pokhran, area of Rajasthan, India. *Bull Environ Contam Toxicol* 86(2):152–158
- Srivastava P, Juyal N, Singhvi AK, Wassson RJ, Bateman MD (2001) Luminescence chronology of river adjustment and incision of Quaternary sediments in the alluvial plain of the Sabarmati River, north Gujarat, India. *Geomorphol* 36(3–4):217–229
- Stallard RF, Edmond JN (1983) Geochemistry of the Amazon-II. The influence and the geology and weathering environment on the dissolved load. *J Geophys Res* 88(14):9671–9688
- Subba Rao N (2006) Seasonal variation of groundwater quality in a part of Guntur District, Andhra Pradesh, India. *Environ Geol* 49:413–429
- Subba Rao N (2008) Factors controlling the salinity in groundwater in parts of Guntur District, Andhra Pradesh, India. *Environ Monit Assess* 138:327–341
- Subramanian V, Saxena K (1983) Hydro-geochemistry of groundwater in the Delhi region of India, relation of water quality and quantity. In: *Proceedings of the Hamburg symposium IAHS publication no. 146*, pp 307–316
- Szabolcs I, Darab C (1964) The influence of irrigation water of high sodium carbonate content of soils. In: *Proceedings of 8th international congress of Isss, Trans, vol 2*, pp 803–812
- Tabios GQ, Salas JD (1985) A comparative analysis of techniques for spatial interpolation of precipitation. *Water Resour Bull* 21:365–380
- Tandon SK, Sareen BK, Rao S, Singhvi AK (1997) Aggradation history and luminescence chronology of Late Quaternary semi-arid sequences of the Sabarmati basin, Gujarat, Western India. *Palaeogeogr Palaeoclimatol Palaeoecol* 128:339–357
- Thorne DW, Peterson HB (1954) *Irrigated soils*. Constable and Company, London
- Todd DK (1980) *Groundwater hydrology*. Wiley, New York, p 535
- Tomczak M (1998) Spatial interpolation and its uncertainty using automated anisotropic inverse distance weighting (IDW)—cross-validation/jackknife approach. *J Geogr Inf Decis Anal* 2:18–30
- US Salinity Laboratory Staff (1954) *Diagnosis and improvement of saline and alkaline soils*. USDA Handbook 60. USDA, Washington
- Vengosh A, Ben-Zvi A (1994) Formation of a salt plume in the coastal plain aquifer of Israel: the Be'er Toviyya region. *J Hydrol* 160:21–52
- Vengosh A, Rosenthal E (1994) Saline groundwater in Israel: it's bearing on the water crisis in the country. *J Hydrol* 156:389–430
- Vengosh A, Spivack AJ, Artzi Y, Ayalon A (1999) Geochemical and Boron, Strontium, and Oxygen isotopic constraints on the origin of the salinity in groundwater from the Mediterranean coast of Israel. *Water Resour Res* 35(6):1877–1894
- Vengosh A, Gill J, Davisson ML, Hudson GB (2002) A multi-isotope (B, Sr, O, H, and C) and age dating study of groundwater from Salinas Valley, California: hydrochemistry, dynamics, and contamination process. *Water Resour Res* 38(1):1–17
- Wilcox LV (1955) *Classification and use of irrigation waters*. US Dept Agric Circ, Washington, DC, p 969
- Yamanaka M, Kumagai Y (2006) Sulfur isotope constraint on the provenance of salinity in a confined aquifer system of the southwestern Nobi Plain, central Japan. *J Hydrol* 325:35–55
- Zaheeruddin, Khurshid S (2004) Aquifer geometry and hydrochemical framework of the shallow alluvial aquifers in the western part of the Yamuna river basin, India. *Water Qual Res* 39(2):129–139